HOKKAIDO UNIVERSITY

| | |
|---|---|
| Title | Water-Resistant Pt Sites in Hydrophobic Mesopores Effective for Low-Temperature Ethylene Oxidation |
| Author(s) | Satter, Shazia S.; Hirayama, Jun; Kobayashi, Hirokazu et al. |
| Citation | ACS catalysis, 10(22), 13257-13268<br>https://doi.org/10.1021/acscatal.0c02816 |
| Issue Date | 2020-11-20 |
| Doc URL | https://hdl.handle.net/2115/83304 |
| Rights | This document is the Accepted Manuscript version of a Published Work that appeared in final form in ACS Catalysis, copyright c American Chemical Society after peer review and technical editing by the publisher. To access the final edited and published work see https://pubs.acs.org/doi/10.1021/acscatal.0c02816 . |
| Type | journal article |
| File Information | Supporting Information_200914.pdf, Supporting Information |

Hokkaido University Collection of Scholarly and Academic Papers : HUSCAP

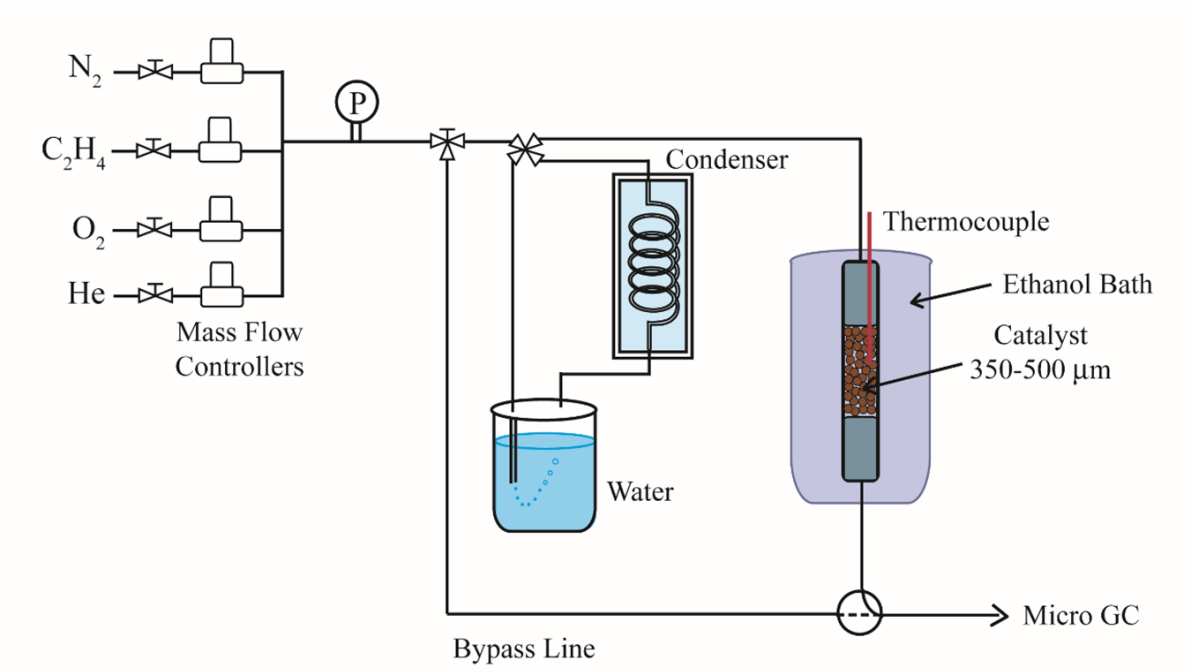
*Supporting Information*

# Water Resistant Pt Sites in Hydrophobic Mesopores Effective for Low Temperature Ethylene Oxidation

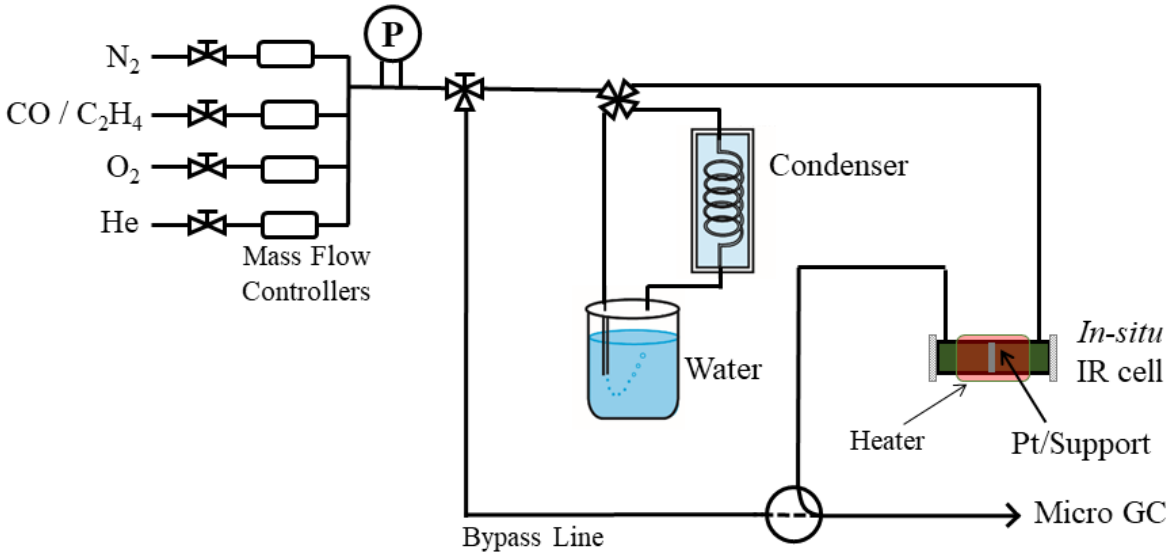
*Shazia S. Satter, Jun Hirayama, Hirokazu Kobayashi, Kiyotaka Nakajima, Atsushi Fukuoka**

Institute for Catalysis, Hokkaido University, Kita 21 Nishi 10, Kita-ku, Sapporo, Hokkaido 001-0021, Japan

Correspondence to Atsushi Fukuoka (fukuoka@cat.hokudai.ac.jp)




**Scheme S1.** Schematic diagram of the fixed-bed flow reactor used for ethylene oxidation.




**Scheme S2.** Schematic diagram of the setup used for the *in-situ* FTIR study.

**Table S1.** Physicochemical properties of Pt/A380 calcined at different temperatures

| Catalyst | $S_{BET}$[a] / $m^2\ g^{-1}$ | V[b]/ $mL\ g^{-1}$ | $D_{Pt}$[c](CO pulse) /nm | $D_{Pt}$[d](XRD) / nm |
|---|---|---|---|---|
| Pt/A380 | 392 | 0.39 | 4.3 | 4.4 |
| Pt/A380(700) | 325 | 0.32 | 4.8 | 2.3 |
| Pt/A380(800) | 313 | 0.32 | 4.9 | 3.8 |
| Pt/A380(900) | 240 | 0.26 | 4.8 | 4.2 |

**a:** BET surface area. **b**: Pore volume estimated using the Barrett−Joyner−Halenda (BJH) Equation. **c**: Average size of Pt nanoparticles estimated by CO chemisorption. **d**: Crystallite size of Pt nanoparticles estimated from (111) diffractions in Figure S1(A) by the Scherrer equation.

**Table S2.** Crystallite size of Pt nanoparticle and catalytic activity for Pt/SBA-15 with different Pt loading.

| **Sample** | **Crystallite Size / nm** | **Normalized $C_2H_4$ Reacted / μmol $g^{-1}$** |
|---|---|---|
| 1% Pt/SBA-15 | 5.0 | 1.72 |
| 1.8% Pt/SBA-15 | 6.2 | 1.83 |

Average Pt size and catalytic activity of two Pt/SBA-15 catalysts with different Pt loading (1.0 wt% and 1.8 wt%) were summarized in Table S2. XRD pattern of these samples showed characteristic diffractions assigned to (111), (200), and (220) of face-centered cubic Pt. Crystallite size of metallic Pt particle was calculated from (111) diffraction using the Scherrer equation for both catalysts, which gave 5.0 nm for 1 wt% sample and 6.2 nm for 1.8 wt% sample. The activity of these catalysts at 300 min of reaction time was also shown in Table S2 after normalization of ethylene converted with Pt weight. Size effect of Pt nanoparticle is of less importance, because the activity for 1.8 wt% Pt/SBA-15 is almost identical to that for 1.0 wt% Pt/SBA-15: 1.0 wt% Pt/SBA-15 for 1.72 μmol $g^{-1}$-Pt and 1.8 wt% Pt/SBA-15 for 1.83 μmol $g^{-1}$-Pt.

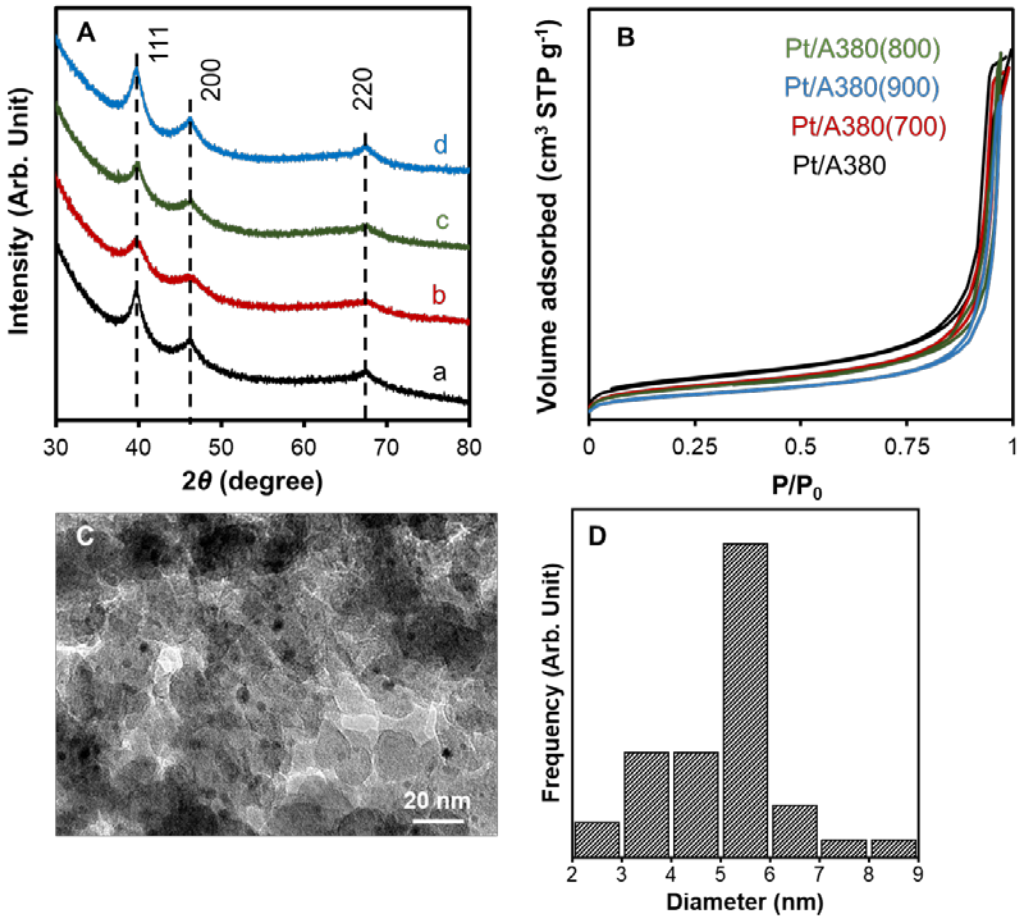



**Figure S1.** (A) XRD patterns (wide-angle) and (B) $N_2$ adsorption isotherms for Pt/A380 samples. (a) Pt/A380, (b) Pt/A380(700), (c) Pt/A380(800) and (d) Pt/A380(900). (C) TEM images and (D) Size distribution of Pt over A380(800) calculated from TEM images.

Silica-supported Pt catalysts were characterized using XRD and $N_2$ adsorption measurements. Figure S1A shows the XRD patterns for the Pt/A380 calcined at different temperatures. Three diffraction peaks appeared at 40°, 46°, and 67° in all catalysts and they are assigned to the (111), (200), and (220) planes of the face-centered cubic (fcc) Pt lattice confirming the successful impregnation of metallic Pt on the supports. $N_2$ adsorption isotherms of Pt/A380 calcined at varying temperature showed a type II isotherm of pronounced hysteresis loop with no significant change among each other.

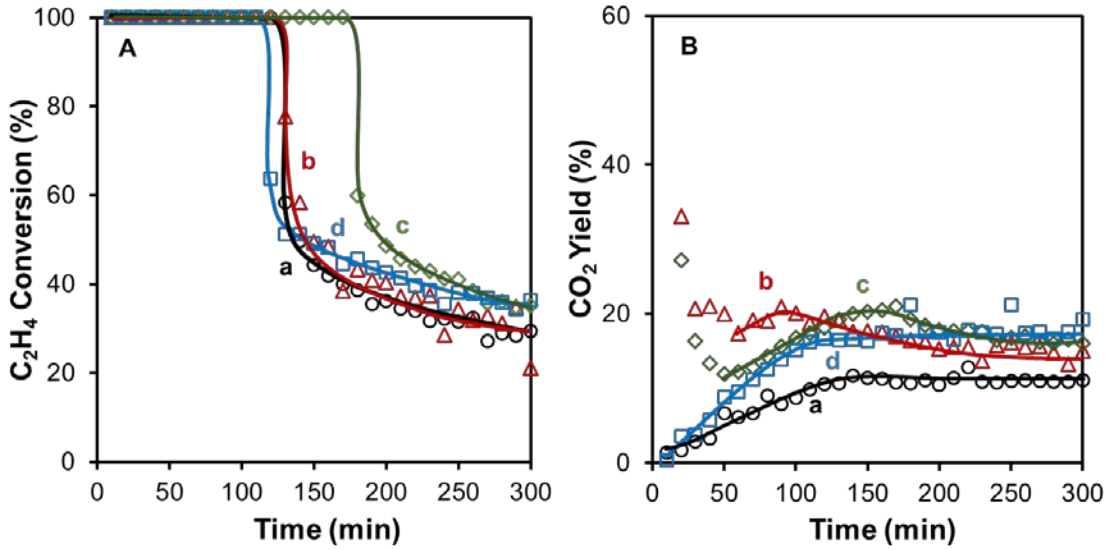



**Figure S2.** Time courses for ethylene conversion (A) and $CO_2$ yield (B) over supported Pt catalysts with bare and calcined A380. Reaction conditions: catalyst 0.4 g (Pt loading 1.8 wt%); SV 1500 mL $h^{-1}$ $g^{-1}$; $C_2H_4$ 50 ppm; $O_2$ 20%; $N_2$ 5%; He (balance); Temp. 0 $^{o}$C. (a) Pt/A380, (b) Pt/A380(700), (c) Pt/A380(800) and (d) Pt/A380(900).

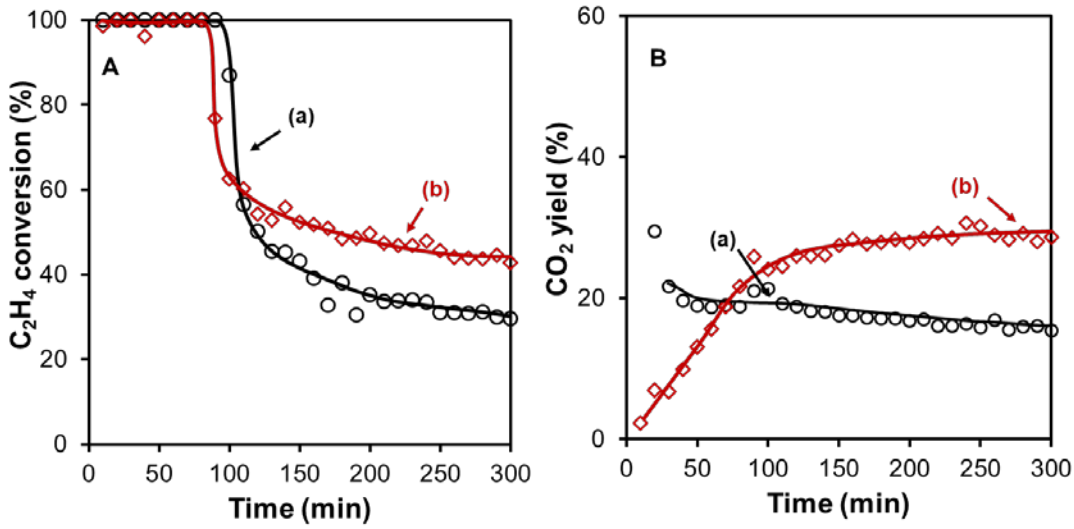



**Figure S3.** Time courses for ethylene conversion (A) and $CO_2$ yield (B) over supported Pt catalysts with bare and calcined SBA-15. Reaction conditions: catalyst 0.4 g (Pt loading 1.8 wt%); SV 1500 mL $h^{-1}$ $g^{-1}$; $C_2H_4$ 50 ppm; $O_2$ 20%; $N_2$ 5%; He (balance); Temp. 0 ºC. (a) Pt/SBA-15 and (b) Pt/SBA-15(800).[1]

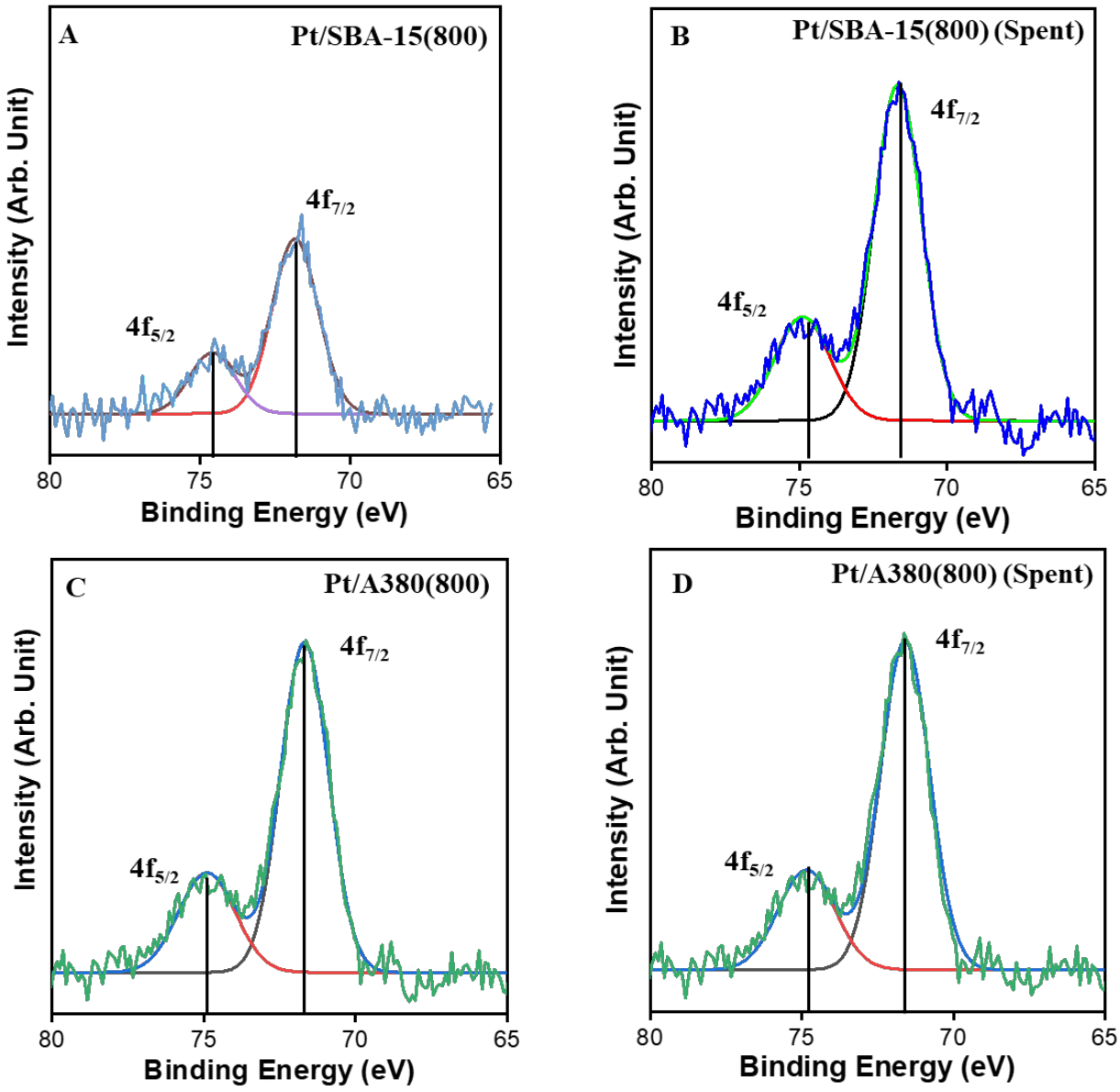



**Figure S4.** XPS spectra of Pt/SBA-15(800) (A), Pt/SBA-15(800) (Spent) (B), Pt/A380(800) (C) and Pt/A380(800) (Spent) (D). The spent catalysts were obtained after 5 h of the reaction at 0 °C.

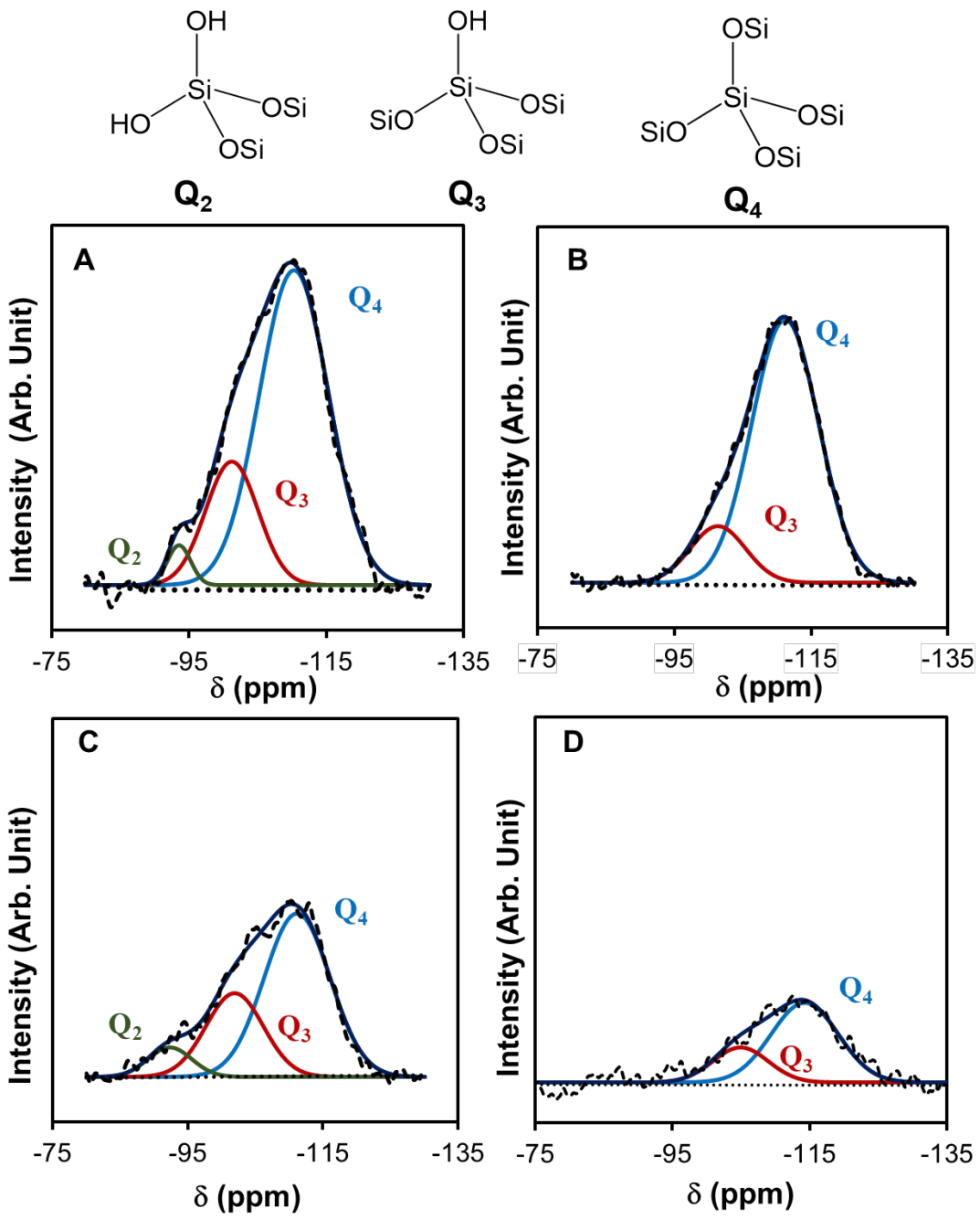



**Figure S5.** $^{29}$Si NMR spectra of Pt/SBA-15 (A), Pt/SBA-15(800) (B), Pt/A380 (C), and Pt/A380(800) (D). $Q_2$, $Q_3$, and $Q_4$ represent $Si(OH)_2(OSi)_2$ and $Si(OSi)_4$, respectively.

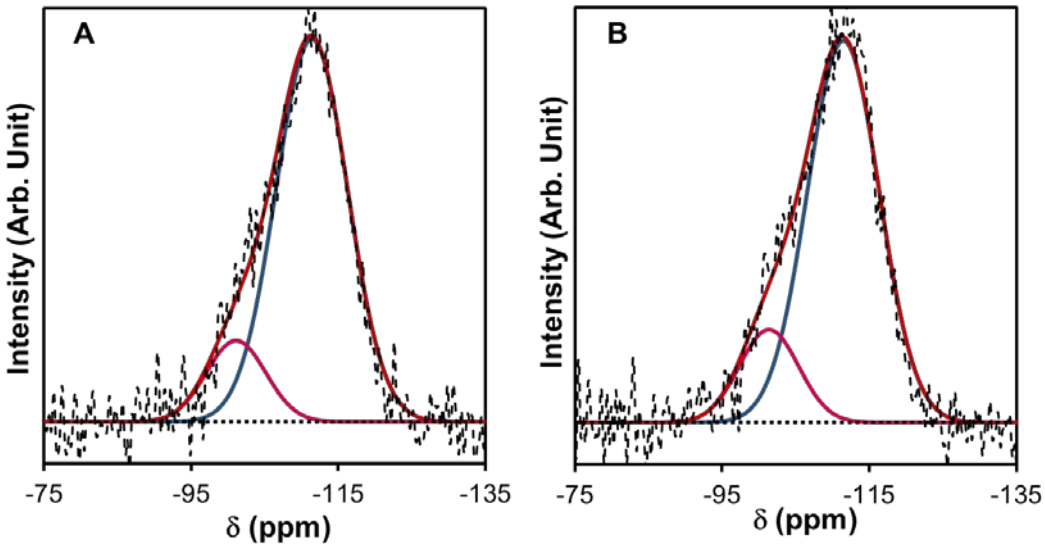



**Figure S6.** $^{29}$Si MAS NMR spectra of Pt/SBA-15(800)-Spent (A) and Pt/SBA-15(800)-Reactivated (B).

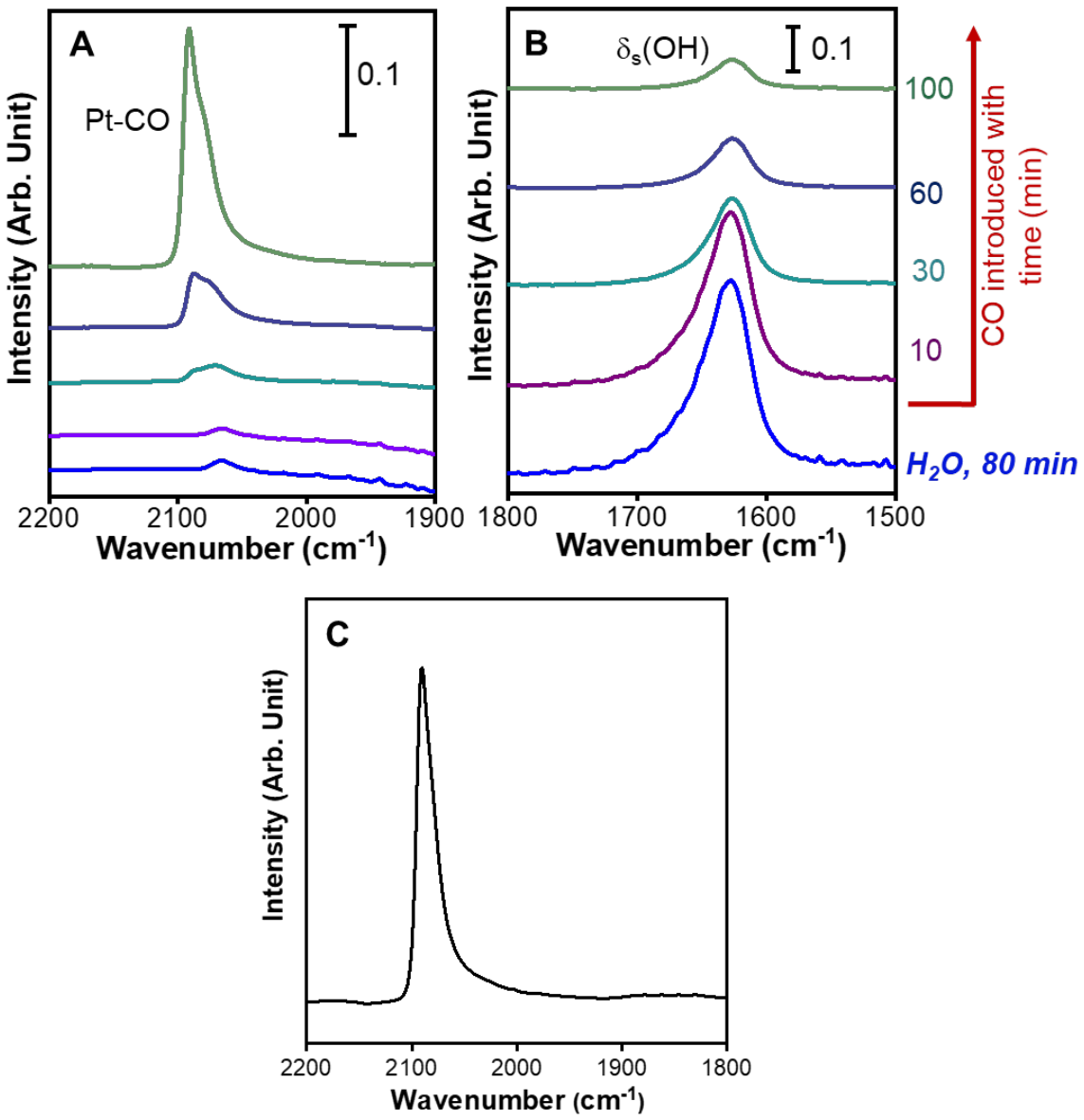



**Figure S7.** Difference FTIR spectra of CO-adsorbed Pt/SBA-15(800) in a stream of dry CO-He gas mixture (CO concentration, 100 ppm). (A) and (B) show Pt–CO band and $H_2O$ bending mode region, respectively. (C) shows the Pt–CO band over dehydrated Pt/SBA-15(800).

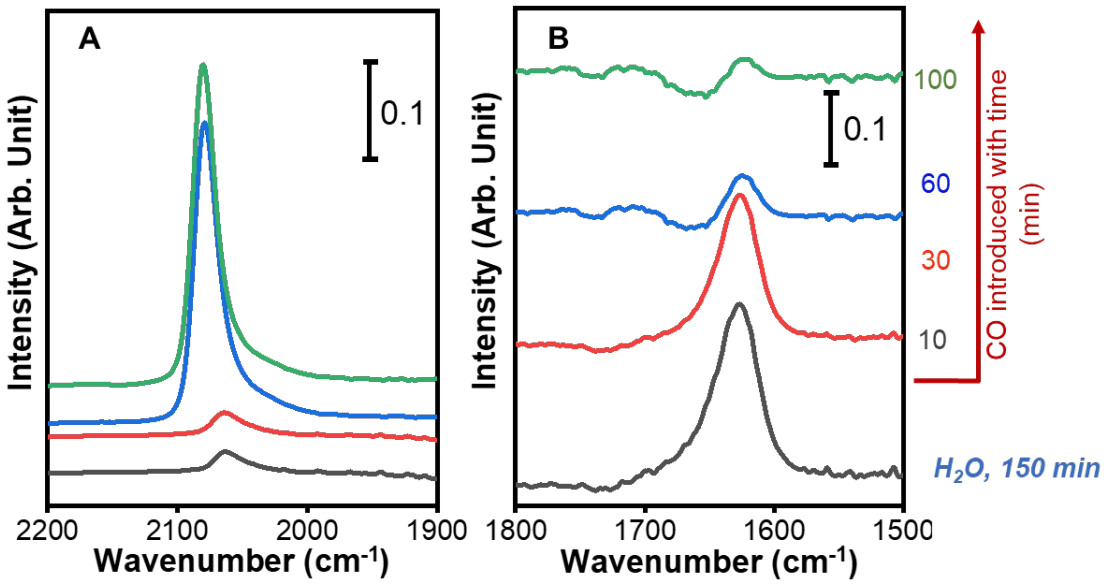



**Figure S8.** Difference FTIR spectra of CO-adsorbed Pt/A380(800) in a stream of dry CO-He gas mixture (CO concentration, 100 ppm). (A) and (B) show Pt–CO band and $H_2O$ bending mode regions, respectively.

**Reference:**

1. Satter, S. S.; Hirayama, J.; Nakajima, K.; Fukuoka, A. Low Temperature Oxidation of Trace Ethylene over Pt Nanoparticles Supported on Hydrophobic Mesoporous Silica. *Chem. Lett.* **2018**, *47*, 1000–1002.